pISSN 1229-3008 eISSN 2287-6251
Progress in Superconductivity and Cryogenics
Vol. 18, No. 4, (2016), pp.25~29
http://dx.doi.org/10.9714/psac.2016.18.4.025

# A compactly integrated cooling system of a combination dual 1.5-MW HTS motors for electric propulsion

**T. D. Le[a, e], J. H. Kim[a], C. J. Hyeon[a], D. K. Kim[b], Y. S. Yoon[c], J. Lee[d], Y. G. Park[d], H. Jeon[d], H. L. Quach[e], and H. M. Kim[a,*]**

[a]*Department of Electrical Engineering, Jeju National University, Jeju, S. Korea*
[b]*Faculty of Wind Energy Engineering, Jeju National University, Jeju, S. Korea*
[c]*Department of Electrical Engineering, Shin Ansan University, Ansan, S. Korea*
[d]*Department of Electrical and Electronic Engineering, Yonsei University, Seoul, S. Korea*
[e]*Department of Electrical, Electronic and Telecommunication Engineering, Can Tho University of Technology, Can Tho, Vietnam*

(Received 12 October 2016; revised or reviewed 16 December 2016; accepted 17 December 2016)

**Abstract**

The high temperature superconducting (HTS) contra-rotating propulsion (CRP) systems comprise two coaxial propellers sited on behind the other and rotate in opposite directions. They have the hydrodynamic advantage of recovering the slipstream rotational energy which would otherwise be lost to a conventional single-screw system. However, the cooling systems used for HTS CRP system need a high cooling power enough to maintain a low temperature of 2G HTS material operating at liquid neon (LNe) temperature (24.5 - 27 K). In this paper, a single thermo-syphon cooling approach using a Gifford-McMahon (G-M) cryo-cooler is presented. First, an optimal thermal design of a 1.5 MW HTS motor was conducted varying to different types of commercial 2G HTS tapes. Then, a mono-cryogenic cooling system for an integration of two 1.5 MW HTS motors will be designed and analyzed. Finally, the 3D finite element analysis (FEA) simulation of thermal characteristics was also performed.

*Keywords*: Cryogenics cooling system, CRP ship propulsion, high temperature superconducting (HTS) motor, thermal characteristics

## 1. INTRODUCTION

Contra-rotating propeller (CRP) is a propulsion configuration offering higher efficiency compared to equivalent single propellers. For marine propulsion applications, CRPs can recover energy from the circumferential flow of the main propeller so they are certainly recognized as the most attractive solution to reduce energy consumption. It has been demonstrated that if a CRP is applied, the propulsion system efficiency can be increased by 15% [1]. Moreover, it is known that the interaction between magnetic flux (iron circuit) and armature current (an electrical circuit) produces the torque, and that torque competes for the same space in the machine determining its volume. Hence, it is considered that applied HTS technology to the synchronous motor for electric propulsion is one of the key issues. It is promising to provide the light weight and compact design with large torque and the iron core can be considerably reduced [2].

Fig. 1 illustrates the most modern electric propulsion system used as a common design theme. It includes significant parts such as a prime mover to drive an HTS generator, cable and switchboards to distribute the generated power, variable speed drive, torque, and acceleration of the propulsion motor [3].

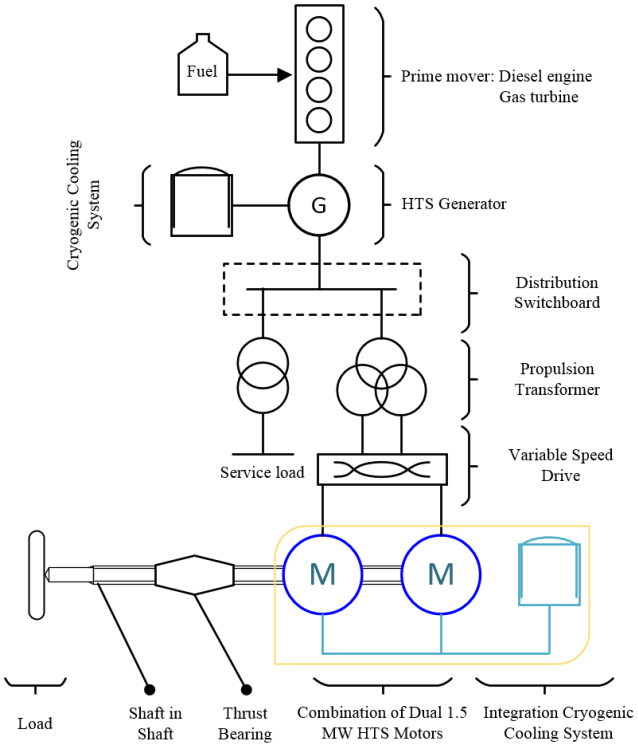


Fig. 1. A basic configuration of an electric propulsion system applied HTS motors [3].

* Corresponding author: hmkim@jejunu.ac.kr

The given baseline system uses an HTS generator and HTS motors to reduce the volume, increase the torque and saving energy. However, that system definitely required a cooling system for HTS generator and motors. Then, an integrated cryogenic cooling system is employed because it has many advantages such as reduction in the number of installed cryo-coolers, increases of energy savings, and improvement of design flexibility. Consequently, the electric propulsion performance will increase the survivability and reliability, and reduce the maintenance and manning requirements.

This paper will optimize the integration cooling system of a dual 1.5 MW HTS motors for electric propulsion. First, the optimal thermal design for a 1.5 MW HTS generator will be performed by using 3 varieties of commercial 2G HTS SuperPower Inc. (SuperPower). Second, a cooling system simulation using a single stage G-M cryocooler for cooling the rotor of the two motors will be performed by applying 3D FEA simulation. The cooling system uses a thermosiphon methodology, which takes into account of single phase LNe, works in a temperature range of 24.5 – 27 K. Finally, other simulations will be also performed to analyze the shaft deformation because of thermal strain during the cooling down the process.

## 2. CONFIGURATION OF CRYOGENIC COOLING SYSTEM

Cryocoolers are the heart of the cooling systems. Reliability and redundancy are important in evaluating a cryocooler and a cooling system. The G-M cryocooler finds widespread application in HTS magnets. It allows the adoption of lower cost commercial compressors which have a mitigation of vibration problems caused by the compressor operation, improvements in reliability and maintenance cost reduction [4]. There is a large commercial availability of G-M cryocoolers [5].

Among the coolants, $H_2$ and $O_2$ are not the preferred options due to the hazards associated with their use. In cases that they are adopted careful monitoring is required. Liquid nitrogen is by far the less costly and more abundant fluid. However, its temperature range restricts its use. Otherwise, liquid neon (LNe) is an attractive refrigerant in bath cooling for rotating machines operating at liquid neon temperature (27 K) [6, 7] because its latent heat of vaporization per volume is 40 times higher than liquid helium. It also has been successfully applied in a recent study [8].

Fig. 2 shows the configuration of a cooling system for a combination of dual 1.5 MW HTS motor using LNe to cool the HTS field coils at 27 K. The cooling system consists of a cryogenic refrigerator, heat exchanger, cryostat and circulation pipe for the LNe flow. At the inlet, LNe at 24.5 K will flow into the rotor. After cooling the HTS coil warmed LNe at maximum 27 K is collected by the cooling pipe. Then, the warmed LNe is cooled again to 24.5 K by a cooling source from G-M cryocooler via a heat exchanger. This cooling process will repeat continuously by using a cryo-pump to maintain the LNe flow.

TABLE I
OPTIMAL PARAMETERS FOR 1.5 MW HTS MOTOR DESIGN WITH DIFFERENT TYPES OF 2G HTS CC.

| | Model 1 SCS4050 | Model 2 SCS6050 | Model 3 SCS12050 |
|---|---|---|---|
| Number of poles | 6 | 6 | 6 |
| Number of SP | 3 | 2 | 1 |
| Operating current [A] | 210 | 315 | 630 |
| HTS length used [km] | 18.22 | 11.986 | 5.768 |
| Coil straight length [mm] | 635 | 635 | 635 |
| Bobbin block length [mm] | 1127 | 1129 | 1133 |
| Rotor inner radius $R_{fi}$ [mm] | 696 | 700 | 706.7 |
| Rotor outer radius $R_{do}$ [mm] | 834 | 834 | 834 |

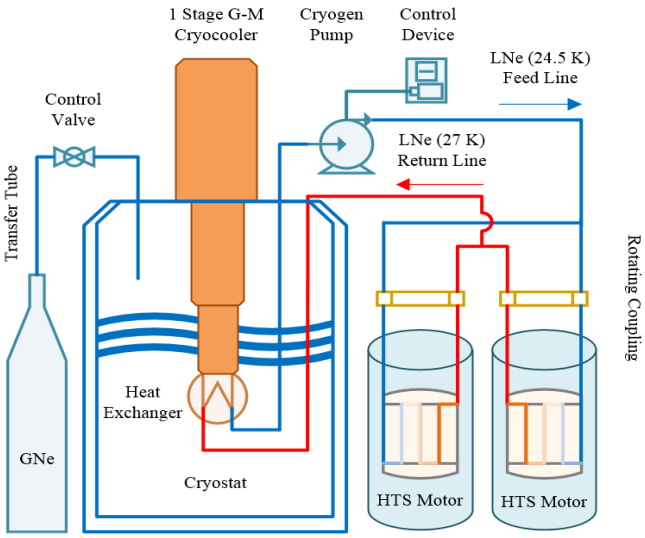


Fig. 2. Configuration of the integrated cryogenic cooling system.

## 3. THERMAL LOSS ESTIMATION VARYING TO DIFFERENT COMMERCIAL 2G HTS TAPES

We propose an optimal thermal design for a 1.5 MW class HTS motor varying to 3 types of commercial 2G HTS. Precisely, the commercial 2G HTS is SCS (surround copper stabilizer) models from SuperPower (SCS4050, SCS6050 and SCS12050, respectively). The winding with the types of 2G CC tape selected in this research has the same thickness of 0.23 mm, including electrical insulating layer, and width of 4, 6, and 12 mm, respectively. These parameters are listed in Table I.

Technically, major rotor losses are 1) current leads loss, 2) torque tube conduction loss, 3) radiation loss and superconducting coil loss from 4) mechanical lap joint Joule heating loss, 5) superconductor index n-value dissipation loss, 6) flux flow in an HTS tape exposed DC transport currents loss and magnetic fields. The total losses due to the combined action of a DC transport current and an external magnetic field proportional to the transport current

and the applied magnetic field to the face of the tape is the sum of the six mentioned losses.

### 3.1. Heat load for the cryogenic system

The cryogenic cooling system is the thermal system which can be more appropriately pictured as a collection of heat leak material connections (mechanical, electrical and fluid) linking the rotating superconducting winding with the stationary room temperature environment. The presence of material links between the cold parts and the outside world introduces a permanent, steady-state, heat load on the superconducting winding volume. These findings delineate the general configuration of the cryogenic cooling system which is composed of three major parts as current leads loss, torque tubes conduction loss and radiation loss.

#### 3.1.1. Current leads loss

Current leads are the connection between the HTS coils and the excitation source. To reduce the conduction heat loss ($Q_c$), for a conduction cooled metal lead operating between room-temperature and cold end temperature (27 K), they are designed based on varying to different diameters. An approximate differential equation for the steady state thermal transfer per unit lead has been derived as follows [9]. Where $T$ and $A$ are the temperature and the cross-section at $z = l$, respectively, while $k(T)$ and $\rho(T)$ are the thermal conductivity and electrical resistivity of material at $T$ temperature, and $I$ is the system operating current.

$$Q_c = \left( k(T) A \frac{dT}{dz} + \rho(T) I^2 \frac{dTdz}{A} \right)\Big|_{z=l} \quad (1)$$

#### 3.1.2. Torque tubes conduction loss

Because of low thermal conductivity ($k$ = 0.53 W/m.K), G-10 material is chosen to design the torque tubes. Considering of its mechanical strength, the transmission torque was designed to be 71.65 kNm (1.5 MW, at 200 rpm, direct driven, 6 poles). The conduction heat leak of the torque tube ($Q_t$) can be calculated as follows [10]. Where $k$ is the thermal conductivity of the material which is dependent on temperature. $\Delta T$, $\delta$, $A$ are the temperature difference, the length of the torque tube and the equivalent cross-sectional area, respectively.

$$Q_t = \frac{kA}{\delta} \Delta T \quad (2)$$

#### 3.1.3. Radiation loss

By wrapping the HTS coil former with superinsulation layers, a significant decrease in radiation heat loss can be achieved. Radiation loss ($Q_r$) between the enclosure and thermal shield is conveniently estimated with the presence of number multi-layer insulation layers $N_i$ [11]. Where $\varepsilon$ is the effective total thermal emissivity of the materials, and $\sigma$ is Stefan-Boltzmann constant. $T_w$ and $T_c$ are the enclosure temperature and thermal shield temperature, respectively.

$$Q_r = \frac{\varepsilon\sigma}{N_i + 1} \left( T_w^4 - T_c^4 \right) \quad (3)$$

### 3.2. Heat losses of superconducting coils

The model of the power losses ($P$) in an HTS tape is intended to be a design tool for an HTS coil used in a power application. To utilize the HTS tape in a power application in an optimal way, it should carry a transport current close to the critical current ($I_c$). At power frequencies and transport currents close to $I_c$ is dominated flux flow losses $Q_{ff}$. Eddy current losses and coupling losses are hence also discussed.

#### 3.2.1. Mechanical lap joint Joule heating loss

It is unavoidable to make joints between the tape length because of the available limitation tape length from manufacturers. Total joint resistance is conveniently estimated maximum 38 nΩ [12]. In consequence, the Ohmic Joule heat loss ($Q_j$) can be easily calculated as follows where there are the number of mechanical joints ($N_j$), operating current ($I$) and joint resistance ($R_j$):

$$Q_j = N_j I^2 R_j \quad (4)$$

#### 3.2.2. Superconductor index $n$-value dissipation loss

Using an index model from [12], index heat dissipation in the HTS tape, $Q_{index}$ may be expressed by:

$$Q_{index} = \int_{total} I_c(B) E_c \left( \frac{I_{op}}{I_c(B)} \right)^{n+1} dl(W) \quad (5)$$

Where $E_c$ is an electric field criterion, e.g., of 1μV/cm to define critical current $I_c$, and $I_{op}$ and $n$ are, respectively, operating current and the index of HTS. In the field dependence in Eq. 6 of superconductor index $n$-value [14], instead the superconductor dependent constant parameters are $n_0 = n(B_a = 0)$, $n_1 = n(B_a >> B_0)$, $B_0$ and $\beta$.

$$n(B_a) = n_1 + (n_0 - n_1) / (1 + B_a / B_0)^{\beta} \quad (6)$$

#### 3.2.3. Flux flow loss

Losses in an HTS tape exposed DC transport currents and parallel magnetic fields. The total power losses due to the combined action of a DC transport current and an external magnetic field proportional to the transport current and applied parallel to the face of the tape is estimated by Eq. 7, and the flux flow losses ($Q_{ff}$) with $N_v$ ($k=k_{//}$) is given by [15]. The quantity $\rho_{ff}$ ($1.15 \times 10^{-24}$ Ω.m) plays the role of flux flow resistivity. While $2a$ and $2w$ are HTS thickness and width, respectively. $N_v(k)$ ($1.34 \times 108$ $m^{-1}A^{-1}$)

TABLE II
THERMAL LOSS ESTIMATION VARYING TO DIFFERENT 2G HTS TAPES [W]

| | Model 1 | Model 2 | Model 3 |
|---|---|---|---|
| Current leads loss | 6.27 | 9.41 | 19.52 |
| Torque tube conduction loss | 4.21/4.8 | 4.24/4.12 | 5.13/4.89 |
| Radiation loss | 11.31/11.26 | 11.32/11.27 | 11.35/11.25 |
| Mechanical lap joint loss | 0.31/0.29 | 0.45/0.42 | 0.87/0.83 |
| n-value index loss | 0.001/0.02 | 0.001/0.07 | 0.09/1.47 |
| Flux flow loss | 0.13/0.12 | 0.77/0.72 | 1.79/1.72 |
| Total loss | 22.23/22.77 | 26.19/26.02 | 38.75/39.68 |

is the number of vortices per unit length and ampere. $N_{v0}$ (76.8x106 $m^{-1}A^{-1}$) is number of pinning centers per unit length and ampere. $I_v$ (4.84 A) is pinning strength, and $I_{op}$ is operating DC current which depends on duration and various current ramp rate.

$$Q_{ff} = \rho_{ff} \frac{I_v^2}{4aw} \exp\left(\frac{N_v(k)}{N_{v0}}\right)\left(\frac{I_{op}}{I_v}\right)^2 \cosh\left(\frac{I_{op}}{I_v}\right) \quad (7)$$

A detailed summary of thermal losses of the cooling system for a 1.5 MW-class HTS rotor is listed in Table II where each loss is shown in detail for each case of commercial 2G HTS applied. Correspondingly, the lowest heat loss is given by Model 1 with an average value at 22.5 W, the largest thermal loss 39.2 W in case of Model 3, the Model 2 is the second position with 26.1 W, respectively.

## 4. CRYOREFRIGERATOR DETERMINATION

The optimal thermal loss estimation is 22.5 W operating at 27 K for one HTS motor Table II. To ensure the thermal shields maintained at 27 K, only one AL330 cryocooler, whose refrigeration capacity approximate 52.5 W @ 24.5 K in Fig. 3, is needed because the total heat loss estimation of field coils from the two HTS motor is 45 W. Therefore, one single stage AL330 cryocooler can sufficiently maintain with over 15.3% margin. The redundant cooling capacity can balance conduction heat leak from the suspension structures of the thermal shield.

Then, a conductive cooling method is employed. The superconducting coils are cooled indirectly by liquid neon (LNe) stored in the coil former which holds the coils. As the LNe and coils are held in the interior and surface of the coil former, respectively, the heat in the coils is dissipated to the coil former by thermal conduction and the heated coil former is cooled by LNe. When the LNe absorbs heat from the coil former, the pipelines collect heated LNe and send them into the heat exchanger where the LNe is cooled again by the cold head. The cooled LNe flows back to the coil former through the pipelines by cryogen pump and begins the next cycle.

In cases of constant surface heat flux, the mean fluid temperature changes linearly in the flow direction because the surface area linearly increases in the flow direction ($A_s$ is equal to the perimeter, which is constant, times the pipe length). The mass flow of LNe is numerically estimated as Eq. 8. Where $m$ is the mass flow, $\Delta T$ is the temperature difference, and $C_p(T)$ is the heat capacity of LNe.

$$\dot{m} = \frac{Q_{total}}{\Delta T \int_{T_i}^{T_f} C_p(T)dT} \quad (8)$$

We also applied the computational approach using the finite element method to simulate the thermal characteristics of cooling process for estimating the transient cooling duration and the deformation of the shaft. Fig.4 shows that with the combination of two HTS motors, the HTS coil will reach steady state operating at 27 K after 109.2 hours. After the steady state operating temperature is reached, the maximum Von Mises stress reached at 7.3x10$^7$ N/m$^2$ in Fig. 5. This result is reliable because it is smaller than the maximum equivalent Mises stress ($\sigma_{eq,m}$ = 7.97x10$^7$ N/m$^2$) estimated by analytical calculation from [16]. Moreover, the shaft was shortened by 10.4 mm because the material was elastic, homogeneous, and isotropic via a linear elasticity approach along with the assumption.

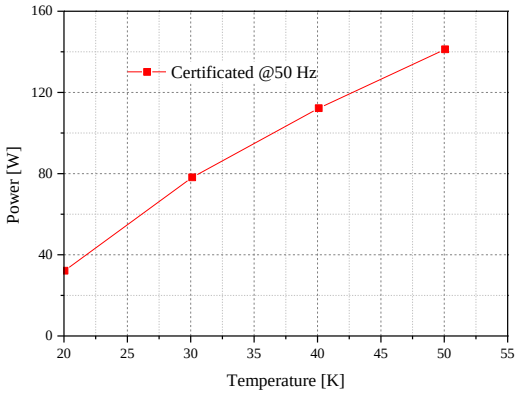


Fig. 3. The single stage cold head capacity profile (AL330).

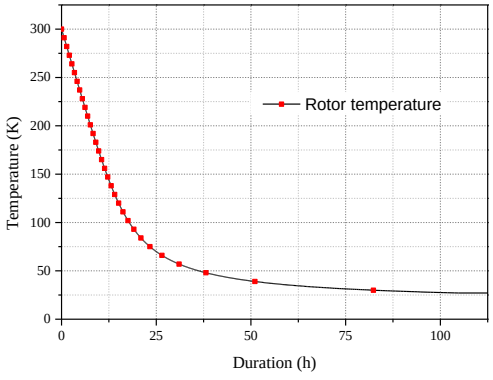


Fig. 4. Thermal transient characteristics simulation result of the cooling system.

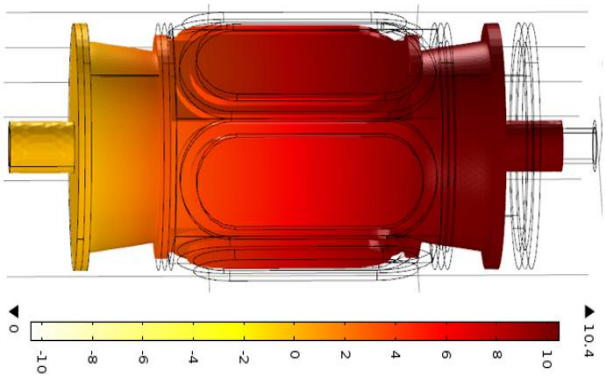


(a)

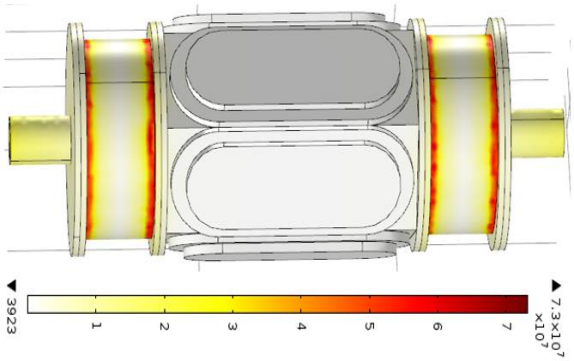


(b)

Fig. 5. Shaft thermal deformation and thermal stress distribution at steady state a) surface of total displacement (mm) and b) surface of Von Mises stress ($N/m^2$).

## 5. CONCLUSIONS

An optimal cooling system is characterized in this study to cool the integration of two HTS motors in CRP electric propulsion. The device's principle application is to take advantage of single phase LNe (24.5 – 27 K) as single thermo-syphon cryogen. Therefore, it can utilize flexibility and availability the cryogen usage in Dewar systems. Because of the significant savings in refrigeration power, cryogen consumption can be achieved with a short investment return time period and at a relatively low cost.

In consideration of using one G-M cryocooler AL330, it was estimated that 0.89 L of LNe used to keep the two HTS rotors, which total optimum heat leak is 45 W, was cooled to 27 K after 4.4 days. At this time, the mass flow rate of cryogen was constantly kept at 17.2 g/s by cryo-pump. Moreover, as the steady state operating temperature was reached, the shaft was shortened by 10.4 mm, and the maximum Von Mises stress reached at $7.3x10^7$ $N/m^2$.

## ACKNOWLEDGMENT

This work was supported by the National Research Foundation of Korea (NRF) grant funded by the Korea government (MSIP) (No. 2016R1A2B4007324).

## REFERENCES

[1] D. Laskos, 'Design and cavitation performance of contra-rotating propeller', Ph.D. thesis, Massachusetts Institute of Technology, 2010.

[2] D. Zhou, Mitsuru, M. Miki, B. Felder, T. Ida, and M. Kitan, "An overview of rotating machine systems with high-temperature bulk superconductors," *Supercond. Sci. Technol.*, vol 25, p. 103001, 2012.

[3] I. Whitelegg, R. Bucknall, "Electrical propulsion in the low carbon economy," Low Carbon Shipping Conference, London, 2013.

[4] A. T. A. M. de Waele, "Basic operation of cryocooler and related thermal machines," *Journal of Low Temperature Physics*, vol. 164, no. 5-6, p. 179236, 2011.

[5] R. Radebaugh, "Cryocoolers: the state of the art and recent developments," *Journal of Physis-Condensed Matter*, vol. 21, pp. 1-9, 2009.

[6] T. Zhang, K. Haran, E. T. Laskaris, and J. W. Bray, "Design and test of a simplified and reliable cryogenic system for high-speed superconducting generator applications," *Cryogenics*, vol. 51, pp. 380-383, 2011.

[7] B. Felder, M. Miki, K. Tsuzuki, N. Shinohara, H. Hayakawa, and M. Izumi, "A 100-W grade closed-cycle Thermosyphon cooling system used in HTS rotating machines," *Advances in Cryogenic Engineering*, vol. 57, pp. 417–424, 2012.

[8] A. R. Kim, K. M. Kim, H. Park, G. H. Kim, T. J. ark, M. Park, S. Kim, S. Lee, H. Ha, S. Yoon, and H. Lee, "Performance analysis of a 10-kW superconducting synchronous generator," *IEEE Trans. Appl. Supercond*. vol. 25, no. 3, p. 5202004, 2015.

[9] T. D. Le, J. H. Kim, S. I. Park, and H. M. Kim, "Conceptual design of current lead for large scale high temperature superconducting rotating machine," *Prog Supercond and Cryo*, vol. 16, no. 2, pp. 54–58, 2014.

[10] T. D. Le, J. H. Kim, S. I. Park, D. H. Kang, H. G. Lee, Y. S. Jo, Y. S. Yoon, and H. M. Kim, "Thermal design of a cryogenics cooling system for a 10 MW class high-temperature superconducting rotating machine," *IEEE Trans. Appl. Supercond*. vol. 25, no. 3, p. 3800305, 2015.

[11] Y. Iwasa, Case Studies in Superconducting Magnets, 2nd ed., Springer, New York, pp. 248-250, 2009.

[12] 2G HTS Wire Specification Overview, http://www.superpower-inc.com/content/wire-specification.

[13] Y. Iwasa, Case Studies in Superconducting Magnets, 2nd ed., Springer, New York, pp. 370-373, 2009.

[14] K. Berger, J. Leveque, D. Netter, B. Douine, and A. Rezzoug, "Influence of temperature and/or field dependences of the E-J power law on trapped magnetic field in bulk YBaCuO," *IEEE Trans. Appl. Supercond*. vol. 17, no. 2, pp. 3028-3031, 2007.

[15] N. Schonborg and S. P. Hornfeldt, "Model of the flux flow losses in a high-temperature superconducting tape exposed to both AC and DC transport currents and magnetic field," *IEEE Trans. Appl. Supercond.*, vol. 11, no. 3, pp. 4078-4085, 2001.

[16] T. Qu, Q. Wu, F. Feng, P. Song, Z. Hong, R. Sun, C. Gu, and Z. Han, "Design and test of a novel thermal insulated torque coupling for a 15-kW fully HTS synchronous generator," *IEEE Trans. Appl. Supercond.*, vol. 26, no. 3, p. 5203105, 2016.